Modeling of Continuous Self-Classifying Spiral Jet Mills Part 1: Model Structure and Validation Using Mill Experiments

Derek Starkey, Cathy Taylor, Nathan Morgan, Katie Winston, and Spyros Svoronos
Dept. of Chemical Engineering, University of Florida, Gainesville, FL 32611

John Mecholsky and Kevin Powers
Dept. of Materials Science and Engineering, University of Florida, Gainesville, FL 32611

Ron Iacocca
Drug Delivery/Device R&D, Eli Lilly and Company, Indianapolis, IN 46221

DOI 10.1002/aic.14642
Published online October 16, 2014 in Wiley Online Library (wileyonlinelibrary.com)

The objective of this work is to develop a milling model for a continuous self-classifying spiral air jet mill. Its foundation is a population balance model with selection and breakage distribution functions that have been related to a minimal number of mill-dependent and powder-dependent parameters. Initially, experimentation is required to determine the mill-dependent parameters for a specific mill, by milling a "base" powder at multiple operating conditions. Powder-dependent parameters can be determined from either mill experiments or from material characterization measurements that require small amounts of powder (presented in Part 2). Ultimately, the milling model presented successfully predicts the product particle size using as inputs the feed particle-size distribution and mill operating conditions. Three crystalline powders, sodium bicarbonate, lactose monohydrate, and sucrose, have been used to test the proposed milling model. © 2014 American Institute of Chemical Engineers *AIChE J*, 60: 4086–4095, 2014
Keywords: particle technology, air jet milling, population balance model, breakage function

Introduction

In the pharmaceutical industry, size reduction techniques are used to improve powder processing and increase the bioavailability of an active pharmaceutical ingredient (API) to obtain the desired therapeutic effect or to aid in drug product formulation. One common size reduction technique used by the industry is air jet milling. Air jet mills are broadly used in the pharmaceutical industry because of their ability to create narrow product size distributions relying on particle–particle impacts to break particles and a simple sanitary design containing no moving parts. As particles are accelerated by gas jets to break upon each other, this mill exhibits minimal contamination compared to other mills which require foreign media or high-speed mechanical parts.

However, there are several challenges in milling. Each powder breaks differently and many pharmaceutical materials, such as APIs, can be very expensive to manufacture and require careful exposure control due to their biological activity. Moreover, during early development phases resources are very limited; therefore, it is undesirable to develop milling model parameters using optimization methods requiring extensive experimentation with large quantities of an API. A model that requires minimal consumption of high-valued powders to establish its parameter values would be advantageous in terms of reducing development costs and exposure risks. Such a model is developed in the present work. The standard batch milling population balance model has been modified to describe and predict the continuous milling of a self-classifying spiral jet mill. The breakage functions of this population balance model include parameters that can be subdivided into two categories: (1) parameters that are independent of the powder being milled and only dependent on the mill characteristics (mill dependent) and (2) mill-independent parameters that depend only on powder characteristics (powder dependent). Thus, the mill-dependent parameter values can be determined for a specific mill through experiments conducted with inexpensive excipient powders, and powder-dependent parameters can be determined either with mill experiments or with small quantities of high-value powders using characterization experiments (described in Part 2).

Population balance models are used to explain the grinding process using two functions: the specific breakage rate (selection function, S_j) and the breakage distribution function, b_{ij}.[1–3] The selection function, S_j, is the probability of a particle of size j breaking in some unit time. The breakage distribution function, b_{ij}, is the fraction of particles breaking from size j to size i. Population balance modeling for batch milling is well defined and has been developed extensively in the literature.[4,5] Also, it has been utilized in modeling mills with internal and external classifiers, but the mill is

This contribution was identified by Priscilla J. Hill (Mississippi State University) as the Best Presentation in the session "Particle Breakage and Comminution Processes" of the 2013 AIChE Annual Meeting in San Francisco, CA.

Correspondence concerning this article should be addressed to D. Starkey at drstarkey4@gmail.com.

usually separated into grinding and classification areas.[6,7] Of the two breakage functions, the selection function has been studied in greater detail in previous literature. The breakage distribution function is often excluded or incorporated in the selection function. This approach is not suitable for every case.[5]

Limited amount of work has been done previously to model air jet mills. Using a loop mill with a closed outlet (batch mode), Nair related breakage parameters to grinding nozzle pressures, nozzle sizes, and material feed rate.[8,9] Likewise, the volumetric flow rate of grinding gas, feed rate, and classification tube height were determined to be the most significant variables in spiral jet mill grinding.[10] There have been many studies using horizontal and vertical jet mills involving different mill sizes, designs, and operating conditions. Midoux et al. completed a great summary of the design and previous work with jet mills, and they expanded it by testing three different sized spiral jet mills with organic crystals.[11]

This work attempts to unite some of the ideas and progress made in the history of mill modeling by developing a simple modeling approach to predict the product size distribution from a continuous spiral jet mill given only the feed composition, mill operating variables (grinding pressure, pusher pressure, and feed rate), and simple material characteristics (see Part 2). This has been done by developing a steady-state population balance model for self-classifying spiral jet mills that does not require separation of grinding and classification zones or complicated residence time distribution models. This method does not assume breakage behavior or relate the breakage distribution function to the probability of breakage. The model presented here is capable of predicting the entire product size distribution with only the feed size distribution, mill operating variables, and simple material characteristics as inputs. The material characterization techniques and connections to powder-dependent parameters are described in Part 2.

Materials and Methods

A typical air jet mill, as shown in Figure 1, has three operating variables: grinding pressure, pusher pressure, and feed rate.[9,10,12] Particles are fed into the feed funnel. The pusher gas enters into the feed apparatus and, using a venturi, creates a partial vacuum at the bottom of the feed funnel which causes the particles to be drawn into the system. The particles are then accelerated by the pusher pressure into the grinding chamber. The grinding gas enters into an outer manifold surrounding the grinding chamber. Grinding nozzles allow the grinding gas to enter tangentially into the grinding chamber at high velocities creating a vortex of gas. Teng et al. and Muller et al. have been able to illustrate this vortex via simulation and experimentation.[12,13] Particles injected into this gas vortex are accelerated toward the grinding chamber walls by centrifugal force. Particles experience multiple impacts with the wall and other particles. A drag force is created by the gases exiting the milling chamber through a central exit. As centrifugal force is proportional to the particle size cubed and drag force is proportional to the particle size squared, as particles break into smaller fragments the centrifugal force decreases faster than the drag force. Depending on the operating variables, there is some given particle size (the cut size) which will be able to leave the grinding chamber. Once a particle breaks down to this

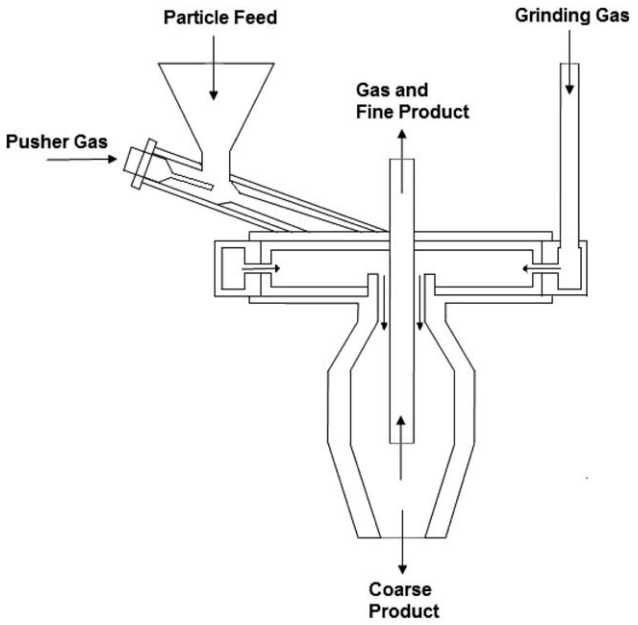

Figure 1. Air jet mill schematic showing gas and particle flows.

critical size, the drag force on the particle will exceed the centrifugal force and the particle will be carried out of the chamber. Therefore, this mill design is said to be self-classifying.

In this work, three common excipient powders were milled. Sodium bicarbonate was obtained from Arm and Hammer®, α-lactose monohydrate was from Foremost Farms® (Product Code 310), and sucrose was provided by Michigan Sugar Company. Material characteristics for all three materials are given in Table 1.

For this study, a Sturtevant 2-in. Micronizer® (see Figure 1), with no liner and stainless steel walls, was used for milling. A nitrogen Dewar was used to supply the carrier gas and the pressures were controlled using valves. The use of nitrogen helped to reduce humidity effects. A model 102M Accurate volumetric screw feeder was used to control the feed rate to the mill. Experiments were completed within defined ranges of the three mill operating variables (grinding pressure, pusher pressure, and feed rate) using a fractional factorial design of experiments. Ten operating conditions were set at three levels of grinding and pusher pressures (30, 65, and 100 psig) and two levels of feed rate (0.050 and 0.100 g/s for lactose and sucrose; and 0.100 and 0.200 g/s for sodium bicarbonate) using the fractional factorial design shown in Table 2.

For each of the operating conditions of Table 2, runs were completed with six different feed compositions, shown in Table 3. The feed compositions in Table 3 were created by sieving original stock powder into corresponding bins and then mixing fractions of each bin together. In summary, each of the three test powders were milled at 10 sets of operating conditions using 6–7 feed compositions for a total of 60–70 experiments per test powder. In the case of sucrose, the as received powder was premilled with the jet mill (operated at a grinding pressure of 30 psig, pusher pressure of 30 psig, and feed rate of 0.400 g/s) to create a new stock powder for experiments.

After the feed was prepared, the volumetric screw feeder was calibrated to feed the powder at the desired feed rate.

Table 1. Material Characteristics of the Three Test Powders Used in This Study

Powder	Sodium Bicarbonate	Lactose Monohydrate	Sucrose
Molecular formula	$NaHCO_3$	$C_{12}H_{22}O_{11}{\cdot}H_20$	$C_{12}H_{22}O_{11}$
Molar mass (g/mol)	84.01	360.31	342.30
Appearance	White crystals	White crystals	White crystals
Crystal structure	Monoclinic	Monoclinic	Monoclinic
Solubility, in IPA	Insoluble	Practically insoluble	Slightly soluble, practically insoluble in dehydrated IPA
D_{10}, as received (microns)	21.0	7.3	25.1
D_{50}, as received (microns)	82.1	66.2	179.0
D_{90}, as received (microns)	155.3	146.7	446.2
Bulk density (g/cm^3)	1.36	0.75	1.11
Particle density (g/cm^3)	2.20	1.53	1.59
Solubility, in water (g/100 mL)	9	22	200
Microindentation hardness (GPa)	0.89	1.06	0.76
Breakage measure (Part 2)	0.39	0.28	0.55
Melting point (°C)	50 (decomposes)	214	186

Once the desired feed rate was achieved, the grinding pressure and pusher pressure were set at the proper levels. Then, the 20-min jet mill procedure commenced. For the first 3 min, the feed was collected into a beaker and weighed to confirm the feed rate. During the next 3 min, six feed rate fractions were collected from the feeder in 30-s intervals to confirm the feed rate was consistent. If the feed rate was incorrect or inconsistent, the feeder would be recalibrated and the process would start again. If conditions were ideal, the feed was allowed to enter the mill continuously for 10 min using nitrogen as the carrier gas. After milling, another six feed rate fractions were collected at 30-s intervals to confirm uniformity of the feed rate over the duration of the mill run. The feeder was then turned off while the mill pressures operated for one additional minute to mill any powder remaining in the mill chamber. Finally, at the 20-min mark, the pressure valves were closed. Then, the mill was carefully and systematically disassembled to collect all the product powder.

After each mill run, powder was collected into three containers: feed, coarse product, and fine product. Material that remained in the feeder was collected as feed. Powder from the product collection chamber, cyclone separator, and grinding chamber was labeled as coarse product. Finally, ultrafine particles found in the piping leading toward and in the filter bag were collected as fine product. Subsequently, a representative sample of each container was sized using a Coulter LS13320 laser diffraction particle-size analyzer using the small volume wet module with isopropanol as a medium. In addition to using the wet module, sonication was used to ensure minimal agglomeration. Powders were analyzed with the Coulter in duplicate or triplicate. The weights and size distributions of the collected coarse product and fine product were used to calculate the size distribution of the combined product. All particle-size distributions and analysis used for modeling were obtained from laser diffraction measurements. The experimental results will be discussed in section Results and Discussion.

Modeling

Population balance model

The model developed here is applicable to self-classification mills such as the spiral jet mill. It makes the following assumptions:

- Particles in any given size class j have the same mean residence time τ_j in the mill.
- Size j breaks the same whether it entered as feed or was created by breakage from a larger particle within the mill.
- The larger the particle the greater the probability of breakage.
- Particles cannot increase in size during milling.

These assumptions are reasonable for isotropic crystalline powders which break in a brittle manner and exhibit minimal effect from fatigue.

For illustration purposes, consider a three-bin system, where Bin 1 is the largest size and Bin 3 is the smallest. The bins are defined such that particles of size 1 are in Bin 1, those of size 2 are in Bin 2, and particles smaller than size 2 are in Bin 3. For our purposes, Bin 3 includes all particles smaller than Bin 2, and therefore, particles cannot break out

Table 2. Jet Mill Operating Conditions from Fractional Factorial Design

Condition Set	Grinding Pressure (psig)	Pusher Pressure (psig)	Feed Rate (g/s)		
Material	All Powders	All Powders	Sodium Bicarbonate	Lactose Monohydrate	Sucrose
A	30	30	0.100	0.100	0.050
B	100	100	0.100	0.100	0.050
C	30	100	0.100	0.100	0.050
D	100	30	0.100	0.100	0.050
E	65	65	0.100	0.100	0.050
F	65	30	0.200	0.050	0.100
G	65	100	0.200	0.050	0.100
H	30	65	0.200	0.050	0.100
I	100	65	0.200	0.050	0.100
J	65	65	0.200	0.050	0.100

Table 3. Jet Mill Feed Compositions According to Sieving

Feed Composition	32–53 Microns (270–450 Mesh) (%)	53–75 Microns (200–270 Mesh) (%)	75–106 Microns (140–200 Mesh) (%)	106–150 Microns (100–140 Mesh) (%)
1	100.00	0.00	0.00	0.00
2	50.00	50.00	0.00	0.00
3	33.33	33.33	33.33	0.00
4	25.00	25.00	25.00	25.00
5	0.00	0.00	100.00	0.00
6	0.00	0.00	0.00	100.00

of Bin 3. σ_j is defined as the probability of size j breaking, and β_{ij} is the probability that size j breaks into size i. These are related to the traditional breakage functions[14] by

$$\sigma_j = S_j \tau_j \tag{1}$$

$$\beta_{ij} = b_{ij} \sigma_j \tag{2}$$

If the mass fractions of each bin in the feed and product are denoted as y_{if} and y_i, respectively, mass balances utilizing the functions σ_j and β_{ij} lead to the following equations

$$y_1 = (1-\sigma_1) \cdot y_{1f} \tag{3}$$

$$y_2 = (1-\sigma_2) \cdot \left[y_{2f} + \beta_{21} y_{1f} \right] \tag{4}$$

$$y_3 = (1-0) \cdot \left[y_{3f} + \beta_{32} y_{2f} + (\beta_{31} + \beta_{32}\beta_{21}) \cdot y_{1f} \right] \tag{5}$$

Particles in Bin 1 that exit the mill must have been fed in Bin 1 and did not break, and as the survival probability is $(1-\sigma_1)$ this leads to Eq. 3. Product particles in Bin 2 can come from unbroken particles from the feed or can be created from particles of size 1 breaking into size 2 (Eq. 4). Finally, particles exiting in Bin 3 can be unbroken size 3 from the feed or particles created by the following mechanisms: Bin 2 feed breaking into Bin 3, Bin 1 feed breaking directly into Bin 3, or breaking from Bin 1 to Bin 2 to Bin 3 (Eq. 5). Obviously, as the number of bins increases the number of σ_j and β_{ij} factors increase. However, not all σ_j and β_{ij} are independent as Eq. 2 implies that

$$\sum_i \beta_{ij} = \sigma_j \tag{6}$$

Thus, the three-bin model has three independent parameters (σ_1, σ_2, and β_{21}) with β_{31} and β_{32} obtained from Eq. 6. In general, if there are n bins, there will be $\frac{n(n-1)}{2}$ independent parameters. To determine σ_j and β_{ij} for a set of mill conditions, (n − 1) experimental runs with single bin feeds would theoretically suffice. For example, with four bins the run with feed in Bin 1 will generate measurements of y_1, y_2, and y_3, and therefore, three equations. The run with Bin 2 feed will give y_2 and y_3, and a run with Bin 3 feed gives only y_3. The resulting six equations can then be used to determine the independent functions σ_1, σ_2, σ_3, β_{21}, β_{31}, and β_{32}.

Chipping conditional probability simplification

In some cases, only breakage to the next bin size or smallest bin size would suffice in describing the breakage of a powder in the spiral jet mill. The rationale for this observation is that in high force impacts, two main mechanisms of breakage typically exist: fragmentation and chipping.[15] Fracture occurs when the largest crack in the greatest stress region propagates to the edges of the particle and creates fragments from impact. Typically, the mechanism of breakage depends on a combination of the kinetic energy and the angle at which a particle impacts. A greater normal force will lead to fragmentation while a greater tangential component will cause chipping. Due to the nature of milling in an air jet mill, which facilitates impacts both between particles and particle-wall collisions, a single breakage mechanism cannot be assumed. However, for the materials used in this study (sodium bicarbonate, lactose monohydrate, and sucrose) this simplifying assumption was tested.

The simplification stated above was implemented in the model as follows: Naming the conditional probability of chipping upon breakage k leads to:

$$\beta_{ij} = \begin{cases} (1-k) * \sigma_j & \text{if } i = j+1 \text{ (next in size bin)} \\ k * \sigma_j & \text{if } i = \text{smallest bin} \\ 0 & \text{any other } i \end{cases} \tag{7}$$

If a particle breaks down utilizing a chipping mechanism, small particles will be removed from a mother particle which will, more than likely, remain in its original bin. On further chipping, the mother particle will eventually fall into the next size bin. Therefore, a single function, k, can define all the β_{ij}. Note that if a particle were to "shatter" such that all fragments end up in the smallest bin, it would fall into the chipping regime. However, as the energy of impact is proportional to the surfaces created, the probability of shattering is much less than that of chipping.

Using the above simplification, for an n-bin system, the number of independent functions is reduced from $\frac{n(n-1)}{2}$ to n. One of the independent functions will always define k while the other $(n-1)$ functions will define σ_1 through σ_{n-1}. Theoretically, only two experiments (with feed containing the largest bin size) are required to determine all the breakage functions for a given set of mill operating conditions.

The sigma function: Probability of breakage in the mill

The following function which relates the probability of size i breaking in the mill, σ_i, to the grinding pressure (GP), pusher pressure (PP), feed rate (FR), and size i (D_i) was developed

$$\sigma_i = \left(\frac{1}{1+\exp(-n)} \right) \tag{8}$$

where

$$n = w_0 + w_{GP} \cdot GP + w_{PP} \cdot PP + w_{FR} \cdot FR + w_{size} \cdot D_i + w_{GPPP} \cdot GP \cdot PP + w_{GPFR} \cdot GP \cdot FR + w_{PPFR} \cdot PP \cdot FR \tag{9}$$

Here, D_i is the volume-weighted mean diameter of Bin i and n can be thought of as a measure of mill energy per particle. The sigmoidal shape of the logistic function mimics typical milling curves and allows for a smooth transition between little to no breakage at low energies and complete breakage (or a $\sigma_j = 1$) at high mill energies. The constant w_0

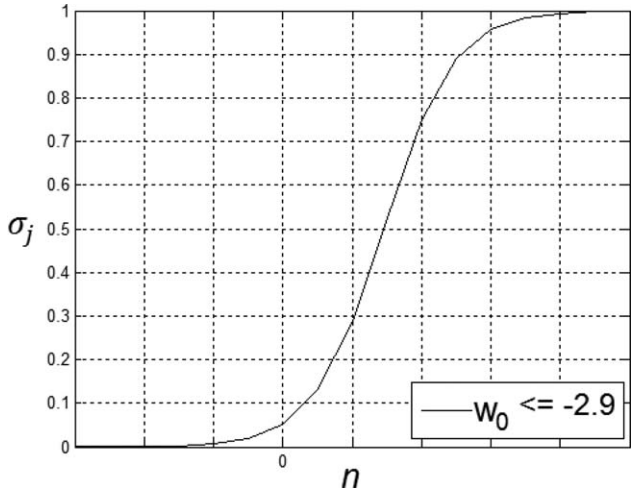

Figure 2. Logistic function used to model the probability of breakage function.

was constrained to be less than or equal to -2.9 to ensure little to no breakage at low mill energy (see Figure 2).

The k function: Conditional probability of chipping on breakage

A function which relates the conditional probability of chipping (given breakage), k, to the grinding pressure, pusher pressure, and feed rate was developed. A modified cosine function was chosen to take advantage of the fact that productive collisions (collisions that cause breakage) at low impact angles will more likely cause chipping while high angle impacts will lead to fragmentation

$$k = \frac{1}{2}\cos(\theta) + \frac{1}{2} \tag{10}$$

where θ is the average productive impact angle

$$\theta = a_0 + a_{GP} \cdot GP + a_{PP} \cdot PP + a_{FR} \cdot FR \tag{11}$$

The modified cosine function allows for a smooth transition between little to no chipping at high angles ($-90°$, using a frame of reference that results in negative angles) and maximum chipping (or a $k = 1$) at low angles (0°). The average productive impact angle, θ, can be linearly related to the energy in the mill. For example, at a given low energy only high angle impacts can actually break the particle, leading to a high angle θ; however, as the energy of the particle increases low-angle impacts start becoming productive and the average productive impact angle moves toward a lower angle.

Model summary

The model developed, illustrated in Figures 3 and 4, predicts the product size distribution from a continuous self-classifying air jet mill using only the feed size distribution and mill operating variables (GP, PP, and FR) given as inputs.

The model can be subdivided into two parts: level 1—six-bin population balance model and level 2—breakage function models. For a specific powder and mill, mill- and powder-dependent parameters can be determined. These parameters and the mill operating variables can be used to predict the breakage functions using the breakage function models presented previously. The breakage functions can then be used in the population balance model to determine the product size distribution exiting the air jet mill from a given feed size distribution.

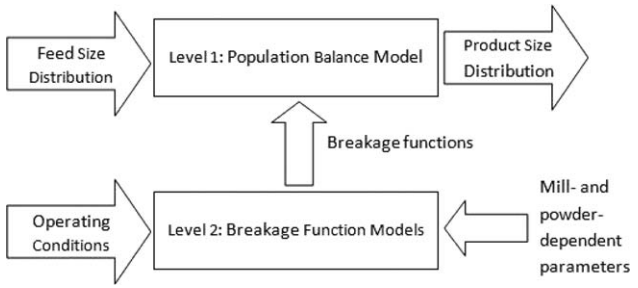

Figure 3. Two-level model architecture.

Results and Discussion

The base test powder was sodium bicarbonate. Sixty jet mill runs were completed at the 10 different mill operating conditions (A–J) and six feed (particle size) compositions (1–6) shown in Tables 2 and 3. An additional 10 repeat runs were made; one per operating condition at feed composition five. For this study, the bins were defined according to Table 4.

Once all runs were completed and mass fractions were calculated, the probabilities of breakage of each bin size (σ_i) and the conditional probability of chipping on breakage (k) were found by fitting the experimental jet mill data to a six-bin population balance model shown in Figure 4. For each set of milling conditions in Table 2, the experimental breakage functions σ_j and β_{ij} or k were determined by minimizing the sum of the squared errors

$$J(\sigma_j, \beta_{ij}) \text{ or } J(\sigma_j, k) = \sum_{r=1}^{6 \text{ or } 7} \sum_{i=1}^{6} \left(y_{r_i,\text{experiment}} - y_{r_i,\text{model}}\right)^2 \tag{12}$$

where y_{r_i} denotes the mass fraction of size i in a run with feed composition r (Table 3). The fit was constrained such that $\sigma_i > \sigma_j$ if $i < j$. This constraint is derived from the fact that larger particles are more likely to break, as it is more probable for them to contain a larger flaw compared to a smaller particle. The larger the flaw the easier it is for that flaw to be propagated and grow into a crack to cause particle fracture. A total of 50 sigmas and 10 k values were found by

POPULATION BALANCE MODEL

KNOWN: $y_{i,exp}, y_{if}$
UNKNOWN: $\sigma_1, \sigma_2, \sigma_3, \sigma_4, \sigma_5, k$

$$y_1 = (1-\sigma_1)\cdot y_{1f}$$

$$y_2 = (1-\sigma_2)\cdot [y_{2f} + \beta_{21} y_{1f}]$$

$$y_3 = (1-\sigma_3)\cdot [y_{3f} + \beta_{32} y_{2f} + (\beta_{31} + \beta_{32}\beta_{21}) y_{1f}]$$

$$y_4 = (1-\sigma_4)\cdot [y_{4f} + \beta_{43} y_{3f} + (\beta_{42} + \beta_{43}\beta_{32}) y_{2f} + (\beta_{41} + \beta_{42}\beta_{21} + \beta_{43}\beta_{31} + \beta_{43}\beta_{32}\beta_{21}) y_{1f}]$$

$$y_5 = (1-\sigma_5)\cdot [y_{5f} + \beta_{54} y_{4f} + (\beta_{53} + \beta_{54}\beta_{43}) y_{3f} + (\beta_{52} + \beta_{53}\beta_{32} + \beta_{54}\beta_{42} + \beta_{54}\beta_{43}\beta_{32}) y_{2f} + (\beta_{51} + \beta_{52}\beta_{21} + \beta_{53}\beta_{31} + \beta_{54}\beta_{41} + \beta_{53}\beta_{32}\beta_{21} + \beta_{54}\beta_{42}\beta_{21} + \beta_{54}\beta_{43}\beta_{31} + \beta_{54}\beta_{43}\beta_{32}\beta_{21}) y_{1f}]$$

$$y_6 = (1-0)\cdot [y_{6f} + \beta_{65} y_{5f} + (\beta_{64} + \beta_{65}\beta_{54}) y_{4f} + (\beta_{63} + \beta_{64}\beta_{43} + \beta_{65}\beta_{53} + \beta_{65}\beta_{54}\beta_{43}) y_{3f} + (\beta_{62} + \beta_{63}\beta_{32} + \beta_{64}\beta_{42} + \beta_{65}\beta_{52} + \beta_{64}\beta_{43}\beta_{32} + \beta_{65}\beta_{53}\beta_{32} + \beta_{65}\beta_{54}\beta_{42} + \beta_{65}\beta_{54}\beta_{43}\beta_{32}) y_{2f} + (\beta_{61} + \beta_{62}\beta_{21} + \beta_{63}\beta_{31} + \beta_{64}\beta_{41} + \beta_{65}\beta_{51} + \beta_{63}\beta_{32}\beta_{21} + \beta_{64}\beta_{42}\beta_{21} + \beta_{65}\beta_{52}\beta_{21} + \beta_{64}\beta_{43}\beta_{31} + \beta_{65}\beta_{53}\beta_{31} + \beta_{65}\beta_{54}\beta_{41} + \beta_{64}\beta_{43}\beta_{32}\beta_{21} + \beta_{65}\beta_{53}\beta_{32}\beta_{21} + \beta_{65}\beta_{54}\beta_{42}\beta_{21} + \beta_{65}\beta_{54}\beta_{43}\beta_{31} + \beta_{65}\beta_{54}\beta_{43}\beta_{32}\beta_{21}) y_{1f}]$$

$$\beta_{ij} = \begin{cases} (1-k)*\sigma_j & \text{if } i = j+1 \\ k*\sigma_j & \text{if } i = 6 \text{ (smallest size bin)} \\ 0 & j+1 < i < 6 \end{cases}$$

Figure 4. Six-bin population balance model equations.

Table 4. Bin Definitions

Bin	Size Range (Microns)	Volume-Weighted Mean Diameter
Bin 1	150–212	186
Bin 2	106–150	132
Bin 3	75–106	93
Bin 4	53–75	66
Bin 5	38–53	47
Bin 6	<38	30

Table 5. Parameters of the Sigma and *k* Functions for Sodium Bicarbonate

Sigma Function		*k* Function	
w_0	−2.90 E+00	a_0	1.45 E+00
w_{GP}	1.09 E−01	a_{GP}	3.72 E−02
w_{PP}	5.92 E−02	a_{PP}	1.41 E−02
w_{FR}	−9.93 E+00	a_{FR}	−3.33 E+00
w_{size}	1.81 E−02		
w_{GPPP}	−8.11 E−04		

fitting the sodium bicarbonate jet mill data to the population balance model.

Using the 50 sigmas for baking soda, the mill-dependent and powder-dependent parameters of the sigma function, Eqs. 8 and 9, were determined by minimizing the sum of the squared differences between the experimental and model σ_j.

The six parameters of the sigma function were obtained by fitting all parameters at the same time, with the constraint that the constant w_0 be less than or equal to −2.9 to ensure little to no breakage at low mill energy. Note that all interactions between operating variables (GP, PP, and FR) were analyzed, and it was determined that, for the three materials studied, the interaction between GP and PP was the only significant interaction between the three possible operating variable interactions (see Figure 5). Thus, only the GP/PP interaction was included in the sigma function (Eq. 9) to minimize the number of parameters.

Similarly, the 10 sodium bicarbonate k values found from the population balance model fits were used to determine the parameters for the k function, Eqs. 10 and 11. However, not all experimental k values are equally reliable. In some cases, where all product particles end up in the smallest bin (Bin 6 for this study), there is no guarantee that the k value found is correct as there can be infinite solutions for k. If all particles of sizes 1, 2, 3, 4, and 5 completely break, then it makes no difference if size 1 breaks sequentially from 1 to 2 to 3 to 4 to 5 to 6 or directly into 6 as in both cases size 6 exits the mill. Therefore, a weighting variable is used to highlight the impact on the model by crucial k values (low pressure conditions with less breakage) and lessen the impact of high breakage k values. The weighting value used is $(1-\sigma_5)^2$ for each condition, where σ_5 is the probability of breakage of particles in the smallest bin size that can break to smaller sizes. Therefore, where σ_5 is close to unity (high breakage) the k value has a lesser effect on the model than where σ_5 is lower. The four parameters of the k function were obtained by fitting all parameters at the same time to minimize the sum of the square differences between experimental and model k values. The mill-dependent and powder-dependent parameters derived from the baking soda fits are shown in Table 5.

In the jet mill, an increase in grinding or pusher pressures will lead to an increase in particle velocity and higher kinetic energy per particle. This will lead to a greater breakage probability, hence the parameters w_{GP} and w_{PP} are positive. As particle size increases, the probability of breakage increases ($w_{size} > 0$), because a larger particle:

- has a greater probability of containing larger flaws
- has a larger mass hence a higher kinetic energy
- experiences greater centrifugal force which will keep it in the mill longer than a smaller particle, leading to more opportunities for collisions and breakage

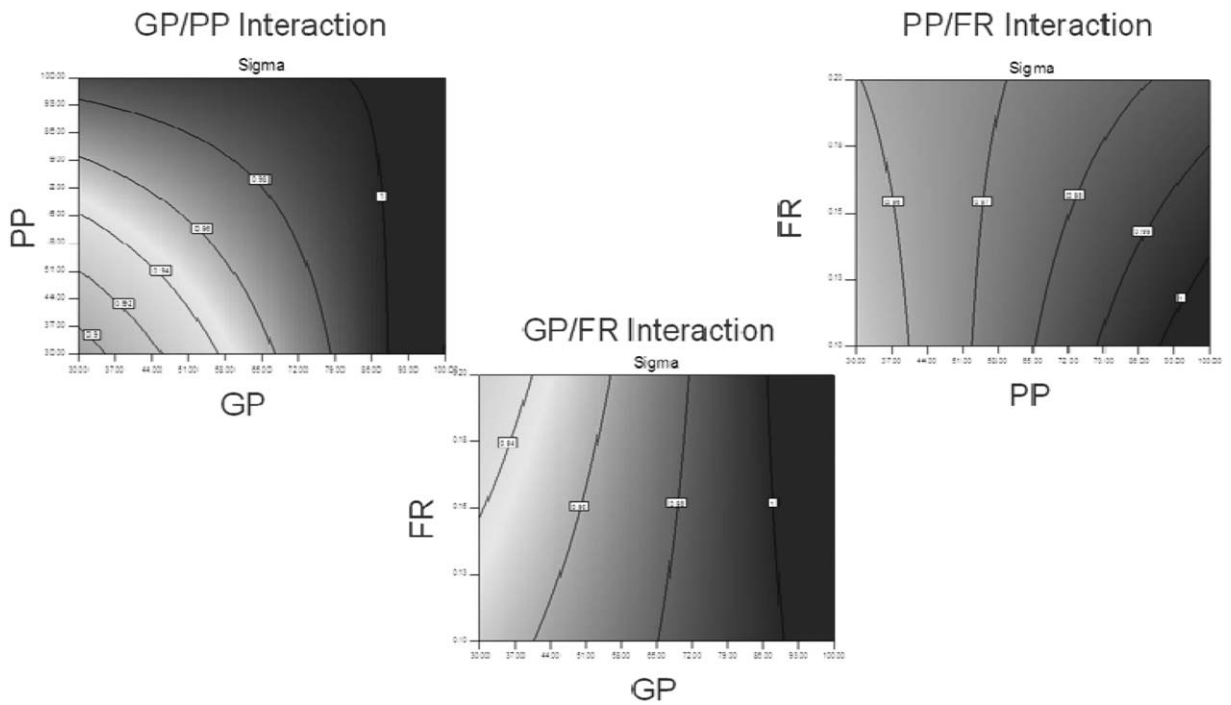

Figure 5. Interaction analysis.

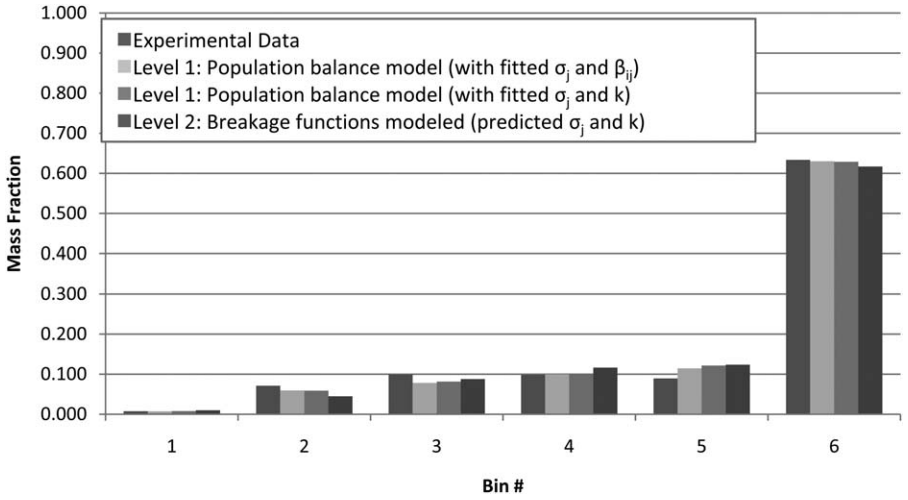

Figure 6. Sodium bicarbonate product from jet mill operated at: grinding pressure of 30 psig, pusher pressure of 30 psig, feed rate of 0.100 g/s, and feed size of 106–150 microns.

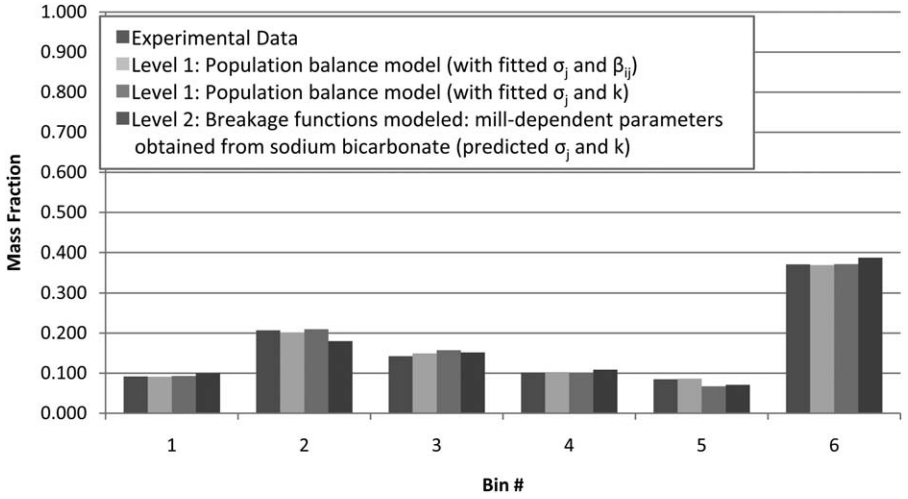

Figure 7. Lactose monohydrate product from jet mill operated at: grinding pressure of 30 psig, pusher pressure of 30 psig, feed rate of 0.100 g/s, and feed size of 106–150 microns.

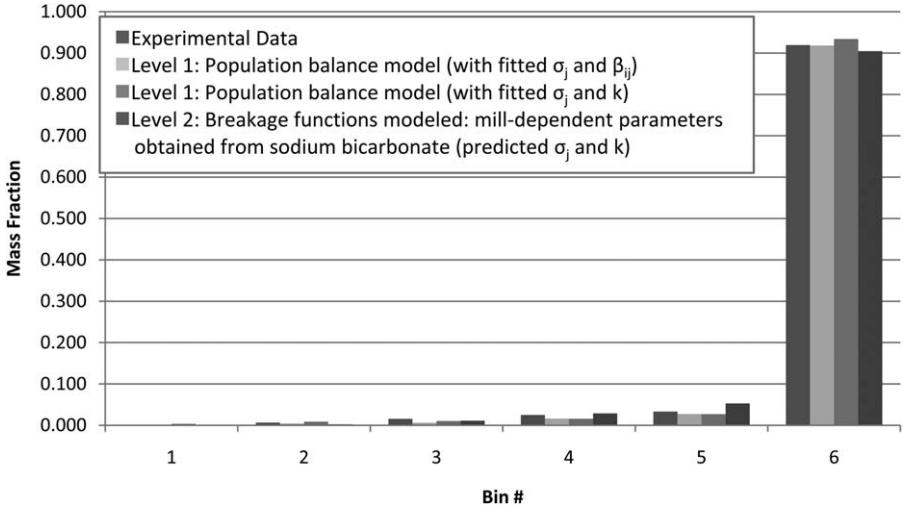

Figure 8. Sucrose product from jet mill operated at: grinding pressure of 30 psig, pusher pressure of 30 psig, feed rate of 0.050 g/s, and feed size of 106–150 microns.

If the feed rate of particles to the mill is increased, the probability of breakage will decrease ($w_{FR} < 0$). More particles will cause the energy provided by the gas to be distributed over a larger number of particles thereby leading to decreased kinetic energy per particle. Finally, the interaction term between GP and PP has a negative effect on the breakage probability which can be explained by an increase in turbulence. When turbulence increases, larger particles can be carried out of the mill without breaking.

Similar to the sigma function, in the jet mill, if either the grinding pressure or pusher pressure is increased, more kinetic energy is supplied to each particle, which will increase the number of small-angle collisions between particles resulting in chipping (a_{GP} and $a_{PP} > 0$). At low energies, or lower grinding and pusher pressure, the low-angle collisions between particles do not generate enough energy to break the particle. If the feed rate increases, more particles are present in the mill which will lead to lower energy per particle. With less energy, only high angle impacts will be productive so θ will be higher and the probability of chipping will decrease leading to $a_{FR} < 0$.

The six parameters determined for sodium bicarbonate were used as an initial guess for fitting lactose and sucrose data. Allowing all parameters to change to minimize the sum of squared differences for each powder, the only parameter that changed substantially was the w_{size} parameter. This parameter is dependent on the material while the constant, w_0, and all the parameters associated with operating variables and interaction terms (w_{GP}, w_{PP}, w_{FR}, and w_{GPPP}) are mill dependent. This makes physical sense as mill operating variables generate energy in the mill independent of the material used while the energy induced on each particle depends on the properties of the material used. Therefore, to limit the number of powder-dependent parameters and still fit the data, all parameters other than w_{size} were fixed to the sodium bicarbonate values and only w_{size} was allowed to change to fit the σ_j of lactose and sucrose. The five mill-dependent parameters are constant for the specific mill used. The w_{size} parameter can be determined from jet mill runs or material characterization (described in Part 2).

Likewise, the k function parameters for sodium bicarbonate were used as an initial guess for lactose and sucrose. Here, the a_0 constant was considered a powder-dependent parameter while the other parameters were fixed at the sodium bicarbonate value. This approach gave minimal degradation between the model and experimental values. Of the four parameters in this model, only a_0 is considered to be powder dependent, because the impact angle at which a particle can break is dependent on the material used. The a_0 parameter can be determined from jet mill runs or material characterization (described in Part 2).

The experimental and modeled mass fractions in each bin of the product powder obtained from a single jet mill run operated with 106–150 micron feed powder, a grinding pressure of 30 psig, a pusher pressure of 30 psig, and a feed rate of 0.100 g/s for sodium bicarbonate and lactose and 0.050 g/s for sucrose are shown in Figures 6–8, respectively.

These mill operating conditions produce the worst level 1 fits and have the richest data with product powder in multiple bins. The differences between the experimental bars and population balance model bars show how well population balance model describes milling. The differences between the population balance model bars and breakage function model bars show the ability to predict the breakage functions with models, related to mill- and powder-dependent parameters. The graphs also show that the k simplification had low impact for each powder tested. For the worst case, between the level 2 model fits and the experimental data for sodium

Table 6. Sodium Bicarbonate Experimental and Modeled Volume Weighted Geometric Mean Diameter of the Product Distributions for All Jet Mill Runs, Reported in Microns

Operating Conditions										
GP (psig)	30		100		30		100		65	
PP (psig)	30		100		100		30		65	
FR (g/s)	0.100		0.100		0.100		0.100		0.100	
Feed	Exp	Model	Exp	Model	Exp	Model	Exp	Model	Exp	Model
1	32.3	33.1	30.0	30.0	30.3	30.4	30.0	30.0	30.1	30.2
2	34.6	35.5	30.0	30.0	30.8	30.6	30.0	30.0	30.1	30.2
3	35.3	36.5	30.0	30.0	30.3	30.7	30.0	30.0	30.2	30.3
4	37.0	36.8	30.0	30.0	30.6	30.7	30.0	30.0	30.2	30.3
5a	39.7	40.0	30.0	30.0	31.4	30.9	30.0	30.0	30.0	30.3
5b	38.2	40.0	30.0	30.0	31.5	30.9	30.0	30.0	30.0	30.3
6	42.6	42.4	30.0	30.0	31.4	31.1	30.0	30.0	30.0	30.3

Operating Conditions										
GP (psig)	65		65		30		100		65	
PP (psig)	30		100		65		65		65	
FR (g/s)	0.200		0.200		0.200		0.200		0.200	
Feed	Exp	Model	Exp	Model	Exp	Model	Exp	Model	Exp	Model
1	30.7	30.7	30.3	30.3	32.7	32.5	30.2	30.0	30.7	30.5
2	30.8	30.9	30.2	30.4	32.9	33.1	30.1	30.1	30.7	30.6
3	31.4	31.0	30.4	30.4	33.6	34.2	30.3	30.1	30.2	30.6
4	31.5	31.1	30.6	30.4	35.1	35.7	30.1	30.1	30.3	30.7
5a	32.5	31.5	30.8	30.5	37.7	38.1	30.0	30.1	31.1	30.9
5b	32.5	31.3	30.4	30.5	37.1	38.4	30.1	30.1	31.3	31.0
6	34.5	31.8	30.7	30.5	41.1	39.7	30.1	30.1	31.0	31.0

Table 7. Lactose Monohydrate Experimental and Modeled Volume Weighted Geometric Mean Diameter of the Product Distributions for All Jet Mill Runs, Reported in Microns

Operating Conditions										
GP (psig)	30		100		30		100		65	
PP (psig)	30		100		100		30		65	
FR (g/s)	0.100		0.100		0.100		0.100		0.100	
Feed	Exp	Model	Exp	Model	Exp	Model	Exp	Model	Exp	Model
1	34.4	34.3	30.0	30.1	30.3	30.3	30.1	30.0	30.5	30.3
2	37.5	37.0	30.0	30.1	30.8	30.9	30.0	30.0	31.0	30.5
3	42.5	41.6	30.0	30.1	31.1	31.6	30.0	30.0	30.7	30.7
4	47.6	46.1	30.0	30.1	31.6	32.0	30.0	30.0	30.9	30.9
5a	57.7	53.5	30.0	30.2	33.3	33.1	30.0	30.1	31.0	31.2
5b	53.6	52.8	30.0	30.2	32.8	33.0	30.0	30.1	31.3	31.2
6	63.8	61.3	30.0	30.2	34.3	34.2	30.0	30.1	31.0	31.5

Operating Conditions										
GP (psig)	65		65		30		100		65	
PP (psig)	30		100		65		65		65	
FR (g/s)	0.050		0.050		0.050		0.050		0.050	
Feed	Exp	Model	Exp	Model	Exp	Model	Exp	Model	Exp	Model
1	30.0	30.1	30.1	30.1	30.8	30.7	30.0	30.0	30.1	30.1
2	30.0	30.3	30.4	30.2	31.5	31.5	30.0	30.0	30.0	30.3
3	30.0	30.5	30.0	30.2	32.0	32.8	30.1	30.0	30.0	30.3
4	30.3	30.6	30.3	30.3	32.6	33.9	30.1	30.0	30.0	30.4
5	31.3	31.0	30.0	30.4	34.0	36.5	30.0	30.1	30.0	30.7
6	30.0	31.3	30.0	30.5	33.5	38.9	30.7	30.1	30.0	30.8

bicarbonate the average difference was 0.018 with a max of 0.035. For lactose monohydrate and sucrose, the average differences between the level 2 model predictions and the experimental data were 0.014 and 0.008, respectively, with max differences of 0.027 and 0.020. These differences are lower than the differences of the base case fitting of sodium bicarbonate.

To condense the data obtained, Tables 6–8 show the experimental and modeled volume-weighted geometric mean diameter of the product distribution for all runs of sodium bicarbonate, lactose monohydrate, and sucrose, respectively. The volume weighted-geometric mean diameters were calculated for each particle-size distribution using the volume-weighted mean diameters of each bin, shown in Table 4.

Table 8. Sucrose Experimental and Modeled Volume Weighted Geometric Mean Diameter of the Product Distributions for All Jet Mill Runs, Reported in Microns

Operating Conditions										
GP (psig)	30		100		30		100		65	
PP (psig)	30		100		100		30		65	
FR (g/s)	0.050		0.050		0.050		0.050		0.050	
Feed	Exp	Model	Exp	Model	Exp	Model	Exp	Model	Exp	Model
1	30.0	30.5	NA	30.0	30.0	30.1	30.0	30.0	30.0	30.0
2	30.9	30.8	NA	30.0	30.1	30.1	30.2	30.0	30.1	30.0
3	30.7	31.1	NA	30.0	30.1	30.1	30.0	30.0	30.1	30.0
4	31.3	31.4	NA	30.0	30.4	30.1	30.0	30.0	30.7	30.0
5	30.4	31.8	NA	30.0	30.9	30.1	30.0	30.0	30.0	30.0
6	31.9	31.9	NA	30.0	30.4	30.1	30.4	30.0	30.1	30.0

Operating Conditions										
GP (psig)	65		65		30		100		65	
PP (psig)	30		100		65		65		65	
FR (g/s)	0.100		0.100		0.100		0.100		0.100	
Feed	Exp	Model	Exp	Model	Exp	Model	Exp	Model	Exp	Model
1	30.1	30.0	NA	30.0	30.3	30.3	30.1	30.0	30.0	30.0
2	30.6	30.1	NA	30.0	30.8	30.3	30.1	30.0	30.5	30.0
3	30.5	30.1	NA	30.0	30.7	30.3	30.1	30.0	30.1	30.0
4	30.6	30.1	NA	30.0	31.1	30.6	30.4	30.0	30.6	30.0
5	30.0	30.1	NA	30.0	31.6	30.7	30.0	30.0	30.0	30.0
6	30.5	30.1	NA	30.0	34.1	30.8	30.0	30.0	30.1	30.0

Conclusions

The modeling of a self-classifying spiral jet mill was studied using a population balance model and separation of mill and material dependence. Using three common pharmaceutical excipient powders, extensive air jet mill experiments were completed to determine mill-dependent and powder-dependent parameters. A population balance model for self-classifying mills was developed and used to measure the probability of breakage of a particle size j (σ_j) and the conditional probability of chipping on breakage (k). Models were then developed to relate these milling model functions to mill operating variables.

This procedure can be applied to any mill type that is self-classifying or equipped with a particle-size classifier. A different mill would require different mill-dependent parameters, which depend on number of nozzles, nozzle angles, chamber size, and other mill characteristics, to be found by running extensive experiments with inexpensive excipient powders. Moving forward, more work is needed to extend this procedure to other mills to further understand the mill-dependent parameters. Also, more materials and a larger range of operating conditions could be used to extend the development and applicability of the milling model.

Acknowledgments

This project is sponsored by Eli Lilly and Company. The authors would like to thank Chris Conners, Amit Ben-Chanoch, Vipul Bansal, Sunil Siddabathuni, Gary Schieffle, and Kerry Johanson for help in completing experiments and Dr. Santiago Tavares for support and guidance.

Notation

β_{ij} = probability size j breaks into size i
σ_j = probability of size j breaking in the mill
θ = average productive impact angle
a_0 = powder-dependent constant in k function
a_{GP} = mill-dependent weight of grinding pressure in k function
a_{PP} = mill-dependent weight of pusher pressure in k function
a_{FR} = mill-dependent weight of feed rate in k function
API = active pharmaceutical ingredient
b_{ij} = breakage distribution function, fraction of particles breaking from size j to size i
D_i = volume-weighted mean diameter of Bin i
FR = feed rate, g/s
GP = grinding pressure, psig
IPA = isopropanol
i or j = bin number
J = sum of error squared
k = conditional probability of chipping on breakage
n = mill energy per particle
n = number of bins
PP = pusher pressure, psig
r = feed composition number
S_j = specific rate of breakage, probability of a particle of size j breaking in some unit time
τ_j = mean residence time of size j particle in mill
w_0 = mill-dependent constant in sigma function
w_{GP} = mill-dependent weight of grinding pressure in sigma function
w_{PP} = mill-dependent weight of pusher pressure in sigma function
w_{FR} = mill-dependent weight of feed rate in sigma function
w_{size} = powder-dependent weight of size i in sigma function
w_{GPPP} = mill-dependent weight in sigma function
y_i = mass fraction of Bin i in product
y_{if} = mass fraction of Bin i in feed

Literature Cited

1. Epstein B. Logarithmico-normal distribution in breakage of solids. *Ind Eng Chem.* 1948;40:2289–2291.
2. Broadbent S, Callcott T. A matrix analysis of processes involving particle assemblies. *Philos Trans R Soc London Ser A*. 1956;249:99–123.
3. Austin L, Shoji K, Bhatia V, Jindal V, Savage K. Some results on the description of size reduction as a rate process in various mills. *Ind Eng Chem Process Des Dev*. 1976;15:187–196.
4. Kapur PC. Kinetics of batch grinding—part B: an approximate solution to the grinding equation. *Soc Min Eng*. 1970;247:309–313.
5. Berthiaux H, Varinot C, Dodds J. Approximate calculation of breakage parameters from batch grinding tests. *Chem Eng Sci*.1996;51:4509–4516.
6. Gommeren H, Heitzmann D, Kramer H, Heiskanen K, Scarlett B. Dynamic modeling of a closed loop jet mill. *Int J Miner Process*. 1996;44–5:497–506.
7. Kis P, Mihalyko C, Lakatos B. Discrete model for analysis and design of grinding mill-classifier systems. *Chem Eng Process*. 2006;45:340–349.
8. Nair P. Breakage parameters and the operating variables of a circular fluid energy mill Part I. Breakage distribution parameter. *Powder Technol*. 1999;106:45–53.
9. Nair P. Breakage parameters and the operating variables of a circular fluid energy mill Part II. Breakage rate parameter. *Powder Technol*. 1999;106:54–61.
10. Tuunila R, Nystrom L. Technical note effects of grinding parameters on product fineness in jet mill grinding. *Miner Eng*. 1998;11:1089–1094.
11. Midoux N, Hosek P, Pailleres L, Authelin J. Micronization of pharmaceutical substances in a spiral jet mill. *Powder Technol*. 1999;104(2):113–120.
12. Teng S, Wang P, Zhu L, Young M, Gogos C. Experimental and numerical analysis of a lab-scale fluid energy mill. *Powder Technol*. 2009;195:31–39.
13. Muller F, Polke R, Schadel G. Spiral jet mills: hold up and scale up. *Int J Miner Process*. 1996;44–5:315–326.
14. Rhodes M. Particle Size Reduction. In: Introduction to Particle Technology – Second Edition. West Sussex: John Wiley & Sons Ltd, 2008:311–335.
15. Meesters GMH. Particle strength in an industrial environment. In: Salman AD, Ghadiri M, Hounslow MJ, editors. Particle Breakage. The Netherlands: Elsevier, 2007:915–940.

Manuscript received Mar. 24, 2014, and revision received Aug. 22, 2014.